Effect of Bismaleimide Reactive Extrusion on the Crystallinity and Mechanical Performance of Poly(lactic acid) Green Composites

Alexis Baltazar-y-Jimenez, Mohini Sain

Faculty of Forestry, Centre for Biocomposites and Biomaterials Processing, University of Toronto, Toronto, Ontario M5S 3B3, Canada

Received 24 May 2011; accepted 23 July 2011
DOI 10.1002/app.35331
Published online 3 November 2011 in Wiley Online Library (wileyonlinelibrary.com).

ABSTRACT: Poly(D-,L-lactic acid) (PDLA) and PDLA-wood pulp fiber injection molded composites were modified with very small amounts (< 1 wt %) of N′-(*o*-phenylene)dimalemide and 2,2′-dithiobis(benzothiazole) by reactive extrusion and their resulting mechanical and thermal properties characterized. The modification produced an increase in the percent crystallinity (X_c), heat deflection temperature (HDT), impact energy, tensile strength, and modulus in PDLA. A significant reduction in the melting temperature (T_m) and an increase in the thermal resistance (T_{max}) were also found. Fourier-Transform infrared spectroscopy (FTIR) suggests the creation of hydrogen bonds, a thiol ester and/or ester bond during the modification. Reactive extrusion of commercially available poly(lactic acid) (PLA) by means of N′-(*o*-phenylene)dimalemide and 2,2′-dithiobis(benzothiazole) provides a low cost and simple processing method for the enhancement of the properties of this biopolymer. © 2011 Wiley Periodicals, Inc. J Appl Polym Sci 124: 3013–3023, 2012

Key words: additives; biofibers; biopolymers; composites; extrusion

INTRODUCTION

Most natural fibers are flexible, with large aspect ratio and high tensile strength. They can be classified according to their origins, specifically if they are extracted from animal, bacterial, mineral or vegetable sources. The low cost, abundance, low density and renewability of cellulose-based fibers synthesized by vegetal (e.g., wood, husks, fruits, seeds, grasses, reeds, bast plants, stalks, canes, leaves and leaf sheaths), bacterial (e.g., *Acetobacter xylinum*, *Rhizobium leguminosarum*, *S. typhimurium*, and *E. coli*), and invertebrate marine animals (e.g., *Microcosmus fulcatus*) has underpinned the development of value-added renewable materials, including microcrystalline cellulose (MCC)-, nanofibrillated cellulose-, and nanocellulose crystal (whisker)-reinforced green composites.

However, technical difficulties still arise during the processing of cellulose fiber-reinforced poly(lactic acid) (PLA) composites, including low fiber dispersion in the polymer matrix; fiber agglomeration because of strong intramolecular and intermolecular hydrogen bonding; low fiber-matrix interfacial adhesion; and thermal degradation due to incompatible processing temperatures between the fiber and the matrix.

In addition, commercially available PLA usually has lower heat deflection temperature (HDT), mechanical properties, and crystallization kinetics than many synthetic engineering polymers, which hinder its use in durable fiber-reinforced composite applications.

A number of plasticizers, coupling agents and impact modifiers have been reported to improve the properties of PLA, e.g., low molecular weight polyethylene glycol (PEG), oligomeric lactic acid (OLA), citrate ester and other plasticizers may be used to improve the elongation and impact strength. The slow crystallization rate and crystallinity of PLA can be improved by means of small amounts (< 2 wt %) of talc, ethylene bis(stearamide) (EBS) and other physical and chemical nucleating agents, by annealing, and by controlling the maximum cooling rate from the melt.[1,2]

Several authors[3–10] have reported an increase in the tensile strength and heat deflection temperature (HDT) of thermoplastic- and thermosetting-based systems after bismaleimide modification, e.g., N,N′-*m*-phenylene bismaleimide; N,N′-bismaleimide-4,4′-

Correspondence to: A. Baltazar-y-Jimenez (alexis.jimenez@utoronto.ca).

Contract grant sponsors: Ontario Biocar Research Initiative (Canada); Mexican Council on Science and Technology (CONACYT-SNI).

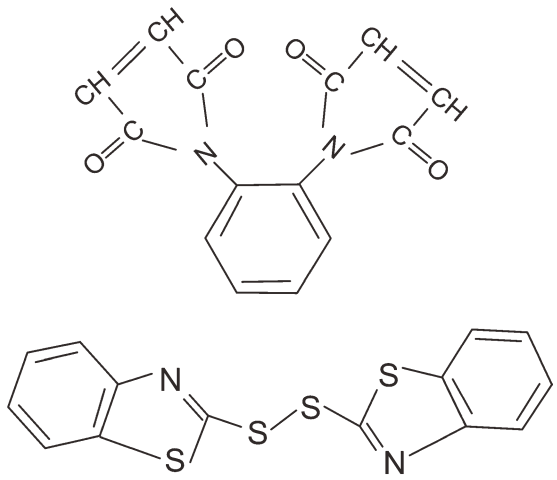

Figure 1 (Top to bottom) Chemical structure of N,N′-(*o*-phenylene)dimalemide and 2,2′-dithiobis(benzothiazole).

diphenylmethane; N,N′-bismaleimide-4,4′- diphenylsulphone, N′-(*o*-phenylene)dimalemide. Bismaleimide contents between 5 and 12 wt %[6,9] were reported. In some cases, the reaction was accelerated by 2,2′ dithiobis(benzothiazole),[11] i.e., a mercaptothiazole class of accelerator used during the crosslinking of rubber. However, the literature lacks of examples of the effect of bismaleimide compounds on PLA and PLA-wood pulp reinforced composites.

In this article, we report on the modification of commercially available poly(lactic acid) and cellulose-based fiber-PLA composites by means of very low amounts (< 1 wt %) of N′-(*o*-phenylene)dimalemide and 2,2′ dithiobis(benzothiazole) by reactive extrusion. The mechanism of adhesion, heat deflection temperature (HDT), impact strength, tensile and flexural properties, melting temperature (T_m) and thermal weight loss after the modification was characterized by chemical analytical techniques. The morphology, chemical composition and average length of wood pulp fibers is also reported.

MATERIALS

Unmodified wood pulp fiber ($\rho = \sim 1.5$ g/cm^3) was kindly provided by GreenCore Composites, (ON, Canada). NatureWorks® Poly(D-,L-lactic acid) (PDLA) 2002D polymer (4% D-lactide, 96% L-lactide content[12]) was obtained from Jamplast, (MO). N′-(*o*-phenylene)-dimalemide and 2,2′ dithiobis(benzothiazole) were obtained from Sigma Aldrich (ON, Canada). Figure 1 depicts the chemical structure of N,N′-(*o*-phenylene)-dimalemide and 2,2′-dithiobis(benzothiazole).

For comparison purposes, a commercially available acrylic impact modifier (Paraloid® BPM-515, Dow Chemical Company) specifically designed for poly(lactic acid) and 3-glycidoxy-propyl-trimethoxy-silane (98% purity, Sigma Aldrich) were selected.

EXPERIMENTAL

Fiber chemical characterization

The chemical composition of the wood pulp fibers was determined by triplicate using standard test methods TAPPI T222 and T203. Soluble lignin content was measured using ultraviolet (UV) absorbance, where the light path is 1 cm and wavelength is 205 nm according to eq. (1):

$$\text{Soluble lignin} = (\text{c v}) \times (1000\ \text{W}_\text{s})^{-1} \times 100 \quad (1)$$

where v is the total volume of filtrate (i.e., 575 mL), W_s the dried weight of the filtrate and c is the lignin concentration in the filtrate. The value of c was calculated from Beer's law using eq. (2):

$$\text{A} = \varepsilon \text{bc} \quad (2)$$

where A is the UV absorbance at 205 nm, ε is the molar absorbtivity (i.e., 110 L/g cm[13]) and b is the path length of the cuvette in which the sample is contained (i.e., 1 cm).

Fiber length determination

The arithmetic mean length of 5000 individual wood pulp fibers was determined by means of the Fiber Quality Analyzer (FQA) (OpTest Equipment, Canada). The procedure is automatically performed by the FQA, which first stirs and suctions a dilute suspension of pulp fibers (< 0.1 g in 500 mL distilled water) and then analyzes them using a high magnification and resolution imaging detection system.

Reactive extrusion and composite production

Predried materials (105°C, 24 h in a standard convection oven) were mixed mechanically prior reactive extrusion. N,N′-(*o*-phenylene)dimalemide (0.75 wt %) and 2,2′ dithiobis(benzothiazole) (0.1 wt %) were extruded with PLA, or PLA and wood pulp to produce composites with twenty percent fiber volume fraction.

A co-rotating twin extruder (Onyx model TEC, Canada) with screw diameter 25 mm, L/D ratio 40 : 1 and eleven heating zones in the temperature range: 180–195°C was utilized for the reactive extrusion. The motor was set at 120 RPM with a feeding rate of 2 kg/h and the extrudate pelletized.

For comparison of the mechanical properties, modified PLA-wood pulp composites with twenty percent fiber volume fraction were modified with Paraloid® BPM-515 (3 wt %) or 3-glycidoxy-propyl-trimethoxy-silane (10 wt %) following the same procedure. Details on the modification are available in the literature.[14]

Standard test specimens were injection molded (Engel ES-28) using a custom-made mold to ASTM D638, D790, and D256 specifications (mold temperature: 20°C; heating zone temperature: 170–180°C; injection time: 8 s; cooling time: 38 s). The tensile test (type I), flexural (127 × 12.7 × 3.2 mm) and impact test (63.5 × 12.7 × 3.3 mm) specimens were stored in a resealable bag and kept in a controlled environment (23°C and 30% relative humidity) until tested. The time elapsed between storing and testing the samples was 72 h.

Differential scanning calorimetry (DSC)

The glass transition temperature (T_g) and melting temperature (T_m) of samples of average weight 10 ± 0.5 mg was calculated in the Differential Scanning Calorimetry (DSC) analyzer (TA Instruments, model Q1000) in the temperature range from −80 to 220°C under nitrogen gas flow (50 mL/min) with a heating ramp of 10°C/min with no annealing time. Only neat PLA was annealed for 24 h at 105°C inside a convection oven.

The percent crystallinity (X_c) was calculated by normalizing the observed heat of fusion to that of 100% crystalline sample from the heating scan of the samples using eq. (3):

$$\text{Percent crystallinity } (\mathrm{X_c}) = 100 \times \frac{\Delta H_m - \Delta H_c}{\Delta H_m^{\infty}} \quad (3)$$

where ΔH_m is the measured endothermic enthalpy, and ΔH_c is the exothermic enthalpy that is absorbed by the polymer crystals during the heating scan. ΔH_m and ΔH_c were determined by integrating the area under the endothermic and exothermic peaks by means of the TA Instruments Universal Analysis Software (v. 4.5). A value of 93.7 J/g was used as the theoretical melting enthalpy of 100% crystalline PLA (ΔH_m^{∞}).[15]

Thermogravimetric analysis (TGA)

The temperature at which maximum weight loss rate occurs (T_{max}) was estimated in the Thermogravimetric Analyzer (TA Instruments, model Q500) in the temperature range 30–600°C under nitrogen gas flow (50 mL/min) and a heating rate of 10°C/min (average sample weight: 10 ± 0.5 mg).

Fourier-transform infrared spectroscopy (FTIR)

The KBr technique was used to obtain the infrared spectra of the samples by means of the FTIR analyzer (Bruker, Tensor 27) in absorbance mode using 40 scans per minute from wavenumber 4000 cm^{-1} to 600 cm^{-1} at a resolution of 4 cm^{-1}. Atmospheric compensation, baseline correction and smoothing (Savitzky-Golay method) were used to reduce noise in the spectra.

X-ray diffraction (XRD)

An automated X-ray generator (Philips, PW 1830) coupled with an X-ray diffractometer controller (Philips, PW 3710) was used to obtain the XRD spectra of the samples. The intensity of the Cu K alpha radiation was measured in the 2θ range from 5° to 40° and step size 0.020° with 2 s count time (λ = 1.5406 Å) at 40 kV and 40 mA.

Tensile and flexural characterization

The tensile and flexural properties of five specimens per sample were measured according to standard test methods ASTM D638 and D790 in the universal testing machine (Instron 3367) (30 kN or 2 kN load and 10 mm/min crosshead speed, respectively). A fixture with cylindrical surfaces with a span of 50 mm was used to perform the flexural test.

Impact resistance characterization

The impact strength of five specimens per sample, notched perpendicularly to the direction of molding, was estimated according to the standard test method ASTM D256 by means of a digital pendulum impact tester (Tinius Olsen 892) equipped with automatic correction for pendulum windage and pendulum-bearing friction.

Heat deflection temperature (HDT)

Injection molded test specimens without annealing and free of defects were used to calculate the heat deflection temperature according to standard test method ASTM D648 with a load of 1.82 MPa (264 psi) applied on top of the specimen vertically and midway using a calibrated apparatus designed for this purpose (CSI 107-M1-252) with a heating rate of 2 ± 0.2°C/min measured by means of a thermocouple.

An arbitrary deformation of 0.25 mm indicates the heat deflection temperature under flexural load in the edgewise position. After each measurement, the apparatus was cooled down by recirculating water until it reached 20°C.

Scanning electron microscopy (SEM)

The fractured surface of gold sputtered specimens (3 min) (Quorum Technologies SC7620, Canada) was analyzed from SEM micrographies (Jeol, model JSM 840) (WD: 32 mm; Acc. Volt.: 15 kV).

RESULTS

Chemical composition of the fiber

Figure 2 shows the average chemical composition of the wood pulp fibers. The similarity in the amount of α-cellulose and hemicelluloses (near 41 wt %) suggests the use of mixed cellulosic sources, such as agricultural or forestry waste, for the production of this pulp.

Many factors have an effect on the chemical composition of cellulose-based fibers, including tree or crop variety; growing conditions and geographical location; climate; fertilization and pruning, which affect the rate of cellulose biosynthesis and early- to late-wood ratio; and cell wall thickness. The separation and extraction method used, including retting, also produces an effect on the quality of the fibers and pulp obtained.

Fiber length analysis

Figure 3 shows the fiber length distribution curve. The arithmetic length of wood pulp fibers is 350 μm, ~ 85% of the fibers analyzed have a length between 50 and 549 μm.

The use of wood pulp fiber as reinforcement in polymer composites is advantageous, mainly due to its availability and low cost. However, it is well known that elementary fibers (ø 10–20 μm) and microfibrils (ø 4–10 nm) usually have greater mechanical properties than technical grade fibers (ø 50–100 μm)[16] and wood pulp fibers (~ ø 20–50 μm), this latter measured from the cross-sectional area of the wood pulp fibers in a SEM micrography.

An improvement in the mechanical properties of cellulosic and lignocellulosic fibers is usually a combination of several factors, including: higher aspect ratio, cellulose content, crystallinity, and molecular weight; and lower microfibril angle. However, the cost involved in separating, extracting and improving the quality of the fibers may be prohibitive from a commercial perspective.

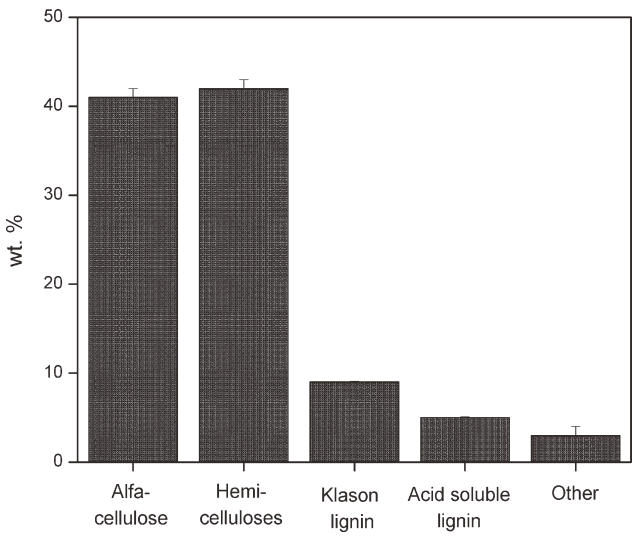

Figure 2 Chemical composition of the wood pulp fibers.

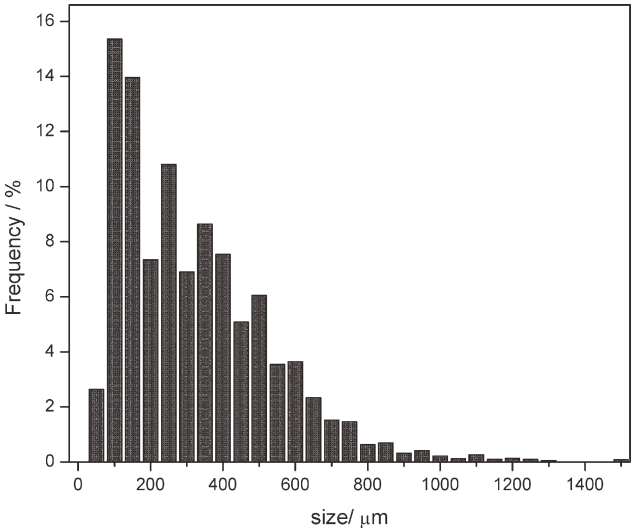

Figure 3 Wood pulp fiber length distribution curve.

Determining the length and length distribution of the reinforcing fibers, as well as the critical fiber length (L_c) in short-fiber reinforced polymer composites allows for better understanding of the performance of this kind of materials. L_c is the minimum fiber length at which the load is completely transferred from the matrix to the reinforcing fiber.

In ideal conditions, the Interfacial Shear Strength (IFSS) is uniformly distributed along the fiber, but: lack of wetting of the fiber by the liquid matrix; poor fiber-matrix interfacial adhesion; fiber discontinuity, misalignment; presence of kinks; and low aspect ratio are some of the factors that have an effect on the amount of stress transferred from the matrix to the fiber.[17]

Despite the IFSS of many natural fibers can be determined by means of the single fiber pull-out test, micro-debonding, fragmentation test and micro-indentation methods, measuring the L_c and IFSS of wood pulp fiber is not plausible due to its low aspect ratio, small fiber length, irregular surface and shape.

Melting behavior, crystallinity, and thermal degradation temperature

Melting behavior

Figure 4 shows the melting temperature (T_m) and glass transition (T_g) of the samples. In this Figure, the PLA sample was annealed. The cold crystallization peak (T_{cc}) of neat PLA 2002D, usually found at 110°C,[18] disappeared after annealing for 24 h at 105°C.

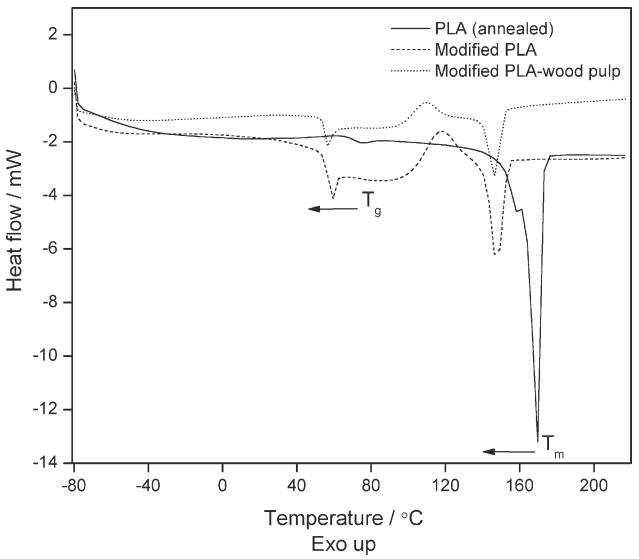

Figure 4 Melting temperature (T_m) and glass transition (T_g). PLA was annealed at 105°C for 24 h in a standard convection oven.

The modification produces a depression in the T_m from 170 to 147°C, and in the T_g from 70 to 60°C, if compared with neat PLA. The most probable explanation is that thermal-oxidative degradation occurs during processing, which produces chain scission and free-radicals with long bulky side groups, which crosslink. This is further discussed in Infrared spectrometry section.

It is known that long bulky side groups disrupt chain packing and induce chain mobility.[19–21] This explains both the reduction in T_m and T_g, respectively.

In addition, the creation of strong dipolar and hydrogen-bonding interactions may account for the T_m depression. Strong dipole-dipole interactions have been reported to reduce the melting temperature in polyimide systems.[22]

Henton et al.[23] suggested that the presence of defects in the crystal arrangement of PLA may result in a depression of T_m. However, we found an increase in the percent crystallinity (X_c) of the modified PLA, which was confirmed by XRD analysis (XRD spectra section).

The reduction in the T_m is noteworthy since it opens the possibility to reduce the thermal degradation that occurs in cellulose-based fibers during processing with PLA. This may be achieved by modifying the PLA matrix first, and incorporating the thermally sensitive reinforcement during a second processing step at lower processing temperature.

The glass transition temperature (T_g) marks the onset temperature at which the chains of a polymer obtain sufficient thermal energy to move. A reduction in the T_g of the modified PLA favors a reduction in the brittle behavior of this matrix. However, a reduction in the T_g of the PLA-wood pulp composite may also indicate low interfacial interactions.[24]

Crystallinity

The percent crystallinity (X_c) of a semicrystalline polymer has an effect on many important properties, including: brittleness; toughness; modulus; optical clarity; creep; barrier resistance; and melting temperature.

An estimation of the percent crystallinity of Natureworks® PLA 2002D is provided by Byrne et al.,[12] who reported $X_c = 9\%$ as this polymer is predominantly amorphous. After annealing (Differential Scanning Calorimetry section) the percent crystallinity of PLA 2002D increased to $X_c = 56\%$. Harris and Lee[1] also reported an increase in the overall crystallinity of PLA from $X_c = 10$ to 43% as function of mold temperature and optimization of processing conditions.

In comparison, the percent crystallinity of the samples without annealing was much lower, i.e., modified PLA blend ($X_c = 10\%$); unmodified PLA-wood pulp composite ($X_c = 8\%$); modified PLA-wood pulp composite ($X_c = 6\%$). Amorphous polymer matrices with low percent crystallinity values are suitable for fast-degrading applications.

It is plausible that the presence of wood pulp fibers with a significant content of hemicelluloses and lignins, which are predominantly amorphous,[25] restricted the crystallization kinetics of PLA. Furthermore, it is known that the rapid cooling rate that occurs when the polymer melt enters the mold, and low injection cycle times reduce the crystallinity of injection molded PLA.[1]

Thermal degradation temperature

Figure 5 shows the differentiated thermogravimetric (DTG) curve of the samples. The DTG curve is the

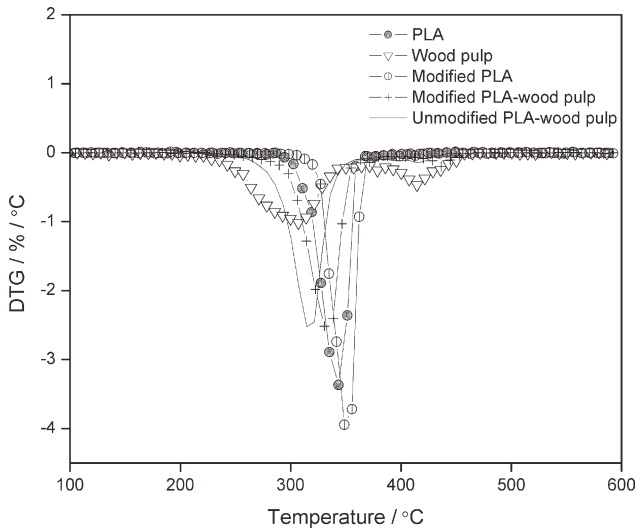

Figure 5 Differentiated thermogravimetric curve.

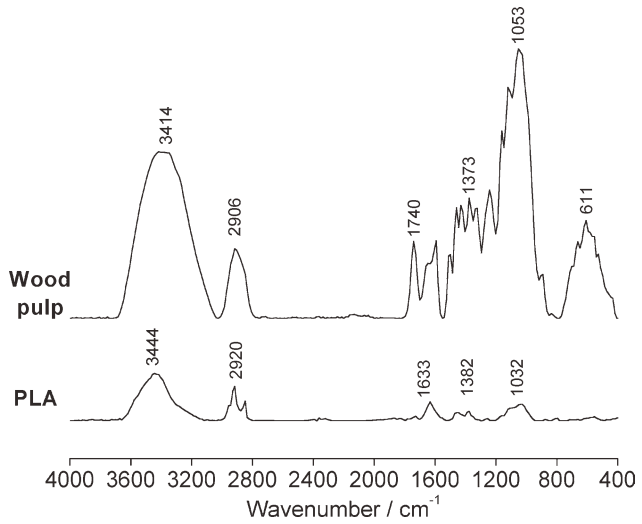

Figure 6 FTIR spectra of wood pulp and PLA.

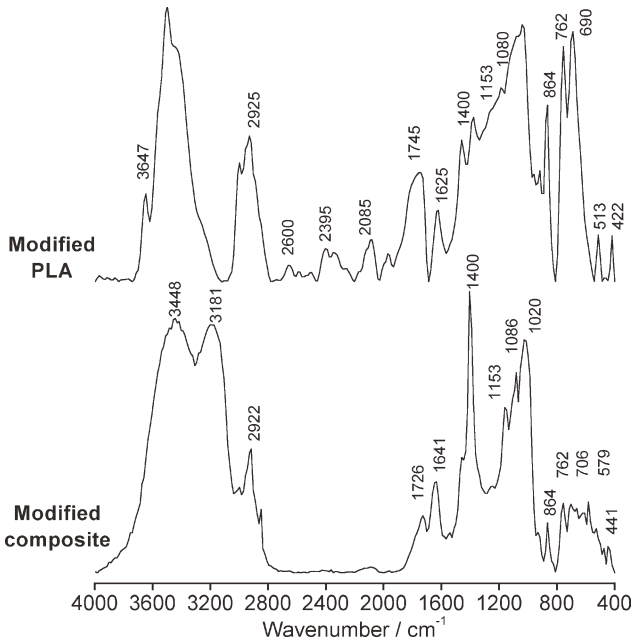

Figure 7 FTIR spectra of modified PLA and modified PLA-wood pulp composite.

first derivative of the weight loss curve as a function of temperature.

The most thermally resistant compounds in cellulosic and lignocellulosic materials are lignins and cellulose, respectively. Two different phases can be identified in the thermogravimetric analysis of the wood pulp fibers after the initial release of moisture in the range 50–100°C (not shown): the depolymerization of cellulose and hemicelluloses (230–350°C) and the degradation of lignins (380–450°C).[26] The pyrolysis of cellulose produces organic compounds, including: α-and β-D-glucose, which suggest that the pyrolysis of cellulose involves an intermediate depolymerization mechanism, as well as levoglucosan; 5-hydroxymethylfurfural; 1,6 anhydro-β-D-glucofuranose; furan and 2-methyl-furan.[27]

TABLE I
Infrared Absorbance Bands Assigned for Wood Pulp, Poly(lactic acid) and N′-(o-phenylene)dimalemide

Material	Assignment	Wavenumber (cm^{-1})
Wood pulp	—OH group vibrations in cellulose & hemicelluloses	4000–2995
	Hydrogen bonds (—OH) in cellulose	3600–3200
	Symmetric CH_2 vibration in cellulose	2940–2850
	H—C—H vibration in hemicelluloses & lignin	2890
	C=O vibration in hemicelluloses	1765–1715
	Aromatic group in lignin	1730–1700
	Hydrogen bonding to C=O	1720–1705
	Absorbed water	1640–1635
	—O—H plane deformation vibration in cellulose	1470–1350
	—CH— deformation vibration in cellulose	1375
	—OH plane deformation vibration	1365–1335
	C–O–C asymmetric vibration	1162–1125
	C—OH vibration in hemicelluloses	1108
	C—O vibration	1060–1015
	Aromatic hydrogen in lignin	900–700
	C—OH out-of-plane bending	670
Imide	Cyclic ureide 5-membered ring	1720
	C=C, C=N stretching	1680–1630
	C—N stretching, N—H bending	1250–1000
PLA	Free —OH stretching	3571
	—CH— stretching (asymmetric & symmetric)	2995, 2944
	Absorbed water	1640–1635
	CH_3— bending	1453
	—CH— bending	1382–1362
	—C—O— stretch	1130

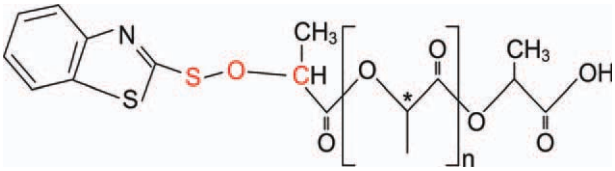

Figure 8 Probable mechanism of adhesion between a moiety of 2,2′ dithiobis(benzothiazole) and poly(lactic acid) by means of a thiol ester bond. [Color figure can be viewed in the online issue, which is available at wileyonlinelibrary.com.]

The temperature at which maximum weight loss rate occurs (T_{max}) increases from 318°C of the unmodified PLA-wood pulp composite to 334°C of the modified PLA-wood pulp composite. However, these values are below the neat PLA matrix (343°C). The presence of thermally sensitive fibers is most probable the reason for the reduced T_{max} found for the composites.

Only the modified PLA matrix has a T_{max} larger than the unmodified matrix, i.e., 351°C. This increase is consistent with the higher percent crystallinity (X_c) found for this sample, which may be due in turn to better packing or polymer chain arrangement.

Infrared spectrometry

Figures 6 and 7 show the infrared absorbance spectra of the unmodified wood pulp and neat PLA, modified PLA and modified wood pulp-PLA composite, respectively. Table I shows the infrared absorbance bands assigned for wood pulp, poly(lactic acid) and N′-(*o*-phenylene)dimalemide.[4,15]

Poly(lactic acid) and wood pulp show strong intermolecular and intramolecular attractions due to the presence of hydroxyl groups. In Figures 6 and 7, the absorbance band 3600–3200 cm^{-1} can be attributed to hydrogen bonds, whereas the band in wavenumber 4000–3600 cm^{-1} suggests the presence of free hydroxyl groups. The latter can be seen in the modified PLA, and may suggest that not all the hydroxyl groups available were modified, possibly because of the very small amounts of N′-(*o*-phenylene)dimalemide and 2,2′ dithiobis(benzothiazole) used.

A thiol ester bond (general structure: *R*-CO-*S*-R′) may be attributed to the absorbance band at 1745–1734 cm^{-1} in Figure 7, whereas the weak absorbance at 2600 cm^{-1} can be assigned to the carbon-bonded sulfhydryl (C-SH) of the thiol group in 2-mercaptobenzothiazole, which results of breaking apart the 2,2′ dithiobis(benzothiazole) molecule during the processing of the modified PLA blend.

The formation of the thiol ester bond (shown in Fig. 8) can occur after cleaving the disulfide bond (*S*-S) in 2,2′ dithiobis(benzothiazole) producing two identical 2-mercaptobenzothiazole moieties each one with a thiol group (-C-SH) capable of binding with available hydroxyl groups or across the double bound of the maleimide moieties in N′-(*o*-phenylene)dimalemide (shown in Fig. 9).

The effect of a bismaleimide compound similar to N′-(*o*-phenylene)dimalemide on the adhesion of wood pulp to polypropylene (PP) was investigated by Sain and Kokta.[4] The creation of a new ester bond (general structure: *R*-COO-R′) between these entities at the interfacial region was argued as the main mechanism of adhesion.

We also found a strong increase in the absorbance band 1300–1000 cm^{-1} in the modified PLA-wood pulp composite (Fig. 7). This absorbance band corresponds to an ester bond as shown by.[28] However, the possibility of the formation of an ether bond (absorbance band: 1270–800 cm^{-1}) between the maleimide moieties of N′-(*o*-phenylene)dimalemide with poly(lactic acid) should not be discarded.

The probable mechanism of interfacial adhesion in the modified PLA-wood pulp composite is shown in Figure 10.

XRD spectra

Figure 11 shows the XRD spectra of the samples. In this Figure, the PLA sample was not annealed. The XRD analysis shows that the spectra of PLA and of the unmodified PLA-wood pulp composite are similar, whereas the spectra of the modified composite is lower. In general terms, lower XRD spectra are

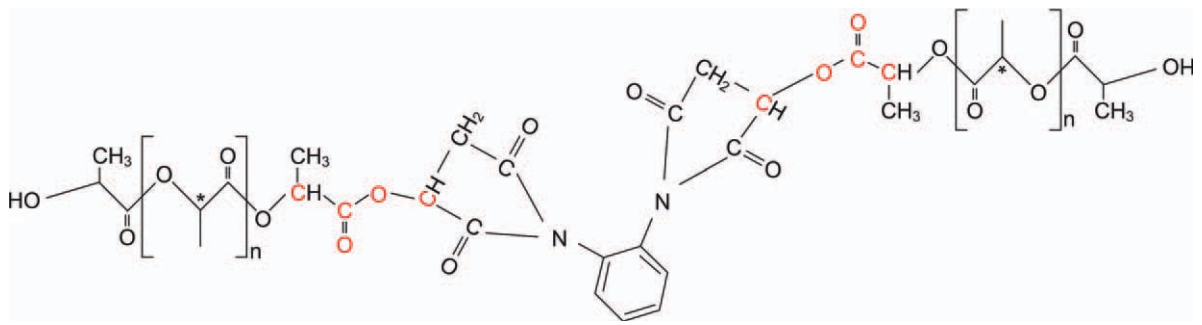

Figure 9 Probable mechanism of adhesion of N′-(*o*-phenylene)dimalemide to poly(lactic acid). [Color figure can be viewed in the online issue, which is available at wileyonlinelibrary.com.]

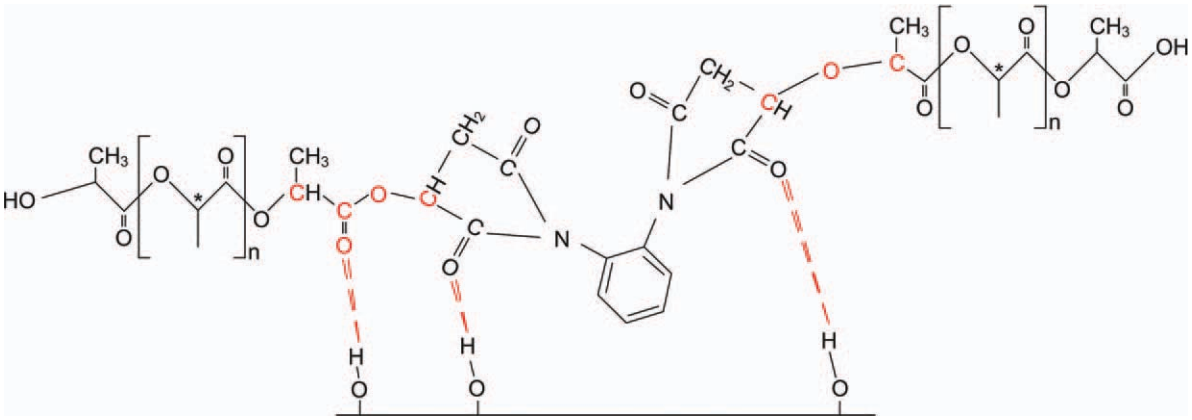

Figure 10 Probable mechanism of interfacial adhesion in the modified PLA-wood pulp composite showing hydrogen bonds (-OH), ester (*R*-COO-R′) and ether bonds (*R*-O-R′). [Color figure can be viewed in the online issue, which is available at wileyonlinelibrary.com.]

related to lower crystallinity values. An increase in the spectra can be seen only for the modified PLA blend. These results are consistent with the percent crystallinity (X_c) results shown in Melting behavior, crystallinity, and thermal degradation temperature section, except for the difference in the thermal history of the PLA sample.

It was expected that the modification would produce an increase in the percent crystallinity of the composite. However, we attributed this result to: (1) the presence of fibers with high hemicelluloses and lignin content, which are predominantly amorphous (Chemical composition of the fiber section); (2) the low crystallization kinetics of PLA 2002 D; and (3) the rapid cooling rate that occurs when the polymer melt enters the mold during composite production, which restricts the crystallization of PLA.

Mechanical properties

Many factors have an effect on the physical and mechanical properties of PLA, including the molecular weight, crystallinity, the configuration of the chiral carbon atom in the repeating molecular structure of PLA, and ratio of D- to L-lactic acid stereoisomers. Commercially available PLA is usually a racemic mixture of D- and D,L-Lactic Acid copolymers (PDLLA).[15]

Table II summarizes the tensile strength and modulus, elongation at break, flexural strength and modulus, impact energy and Heat Deflection Temperature (HDT) of the samples.

Tensile properties

The modification produced a slight increase in the tensile strength and modulus of the modified PLA. However, the introduction of wood pulp reduced the tensile strength if compared with neat PLA, with the exception of the silane-modified composite. The reduction can be explained by a combination of: lack of wetting of the fibers by the matrix; insufficient fiber-matrix interfacial adhesion that reduces the transfer of stress from the matrix to the fibers; poor compatibility between the fibers and the matrix; and the low aspect ratio of the fibers.

The increase in the modulus is due to the introduction of the reinforcing fiber into the matrix, as well as the increase in the crystallinity of PLA after the modification.[1] In addition, during the extrusion process the fibers are exposed to strong shear forces, thereby increasing the contact area of the fibers (i.e., fibrillation), which may favor mechanical interlocking at the fiber-matrix interface that result in higher mechanical properties.[29]

Impact properties

An increase in the impact energy of the samples was found after the modification if compared with neat

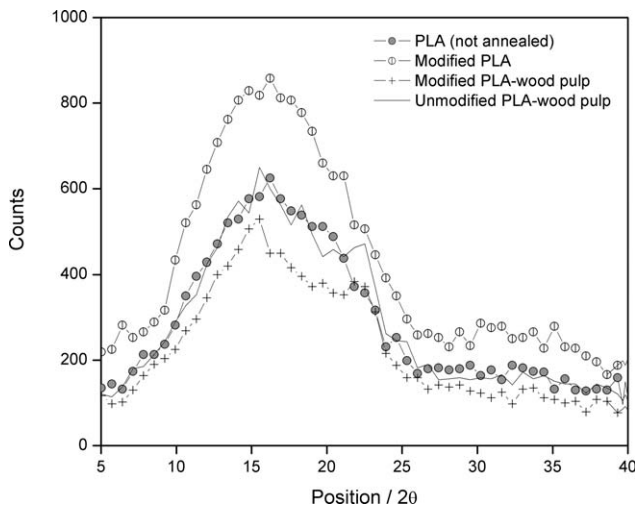

Figure 11 XRD spectra. None of the samples was annealed.

TABLE II
Tensile and Flexural Properties, Impact Energy, and Heat Deflection Temperature (HDT)

Sample	Tensile strength (MPa)	Tensile modulus (GPa)	Elongation at break (%)	Flexural strength (MPa)	Flexural modulus (GPa)	Impact Energy (J/m)	HDT (°C)
PLA	63 (±1.1)	2.5 (± 0.5)	3.0 (±0.1)	106 (+0.4)	2.9 (+0.1)	22.0 (±0.5)	39 (±0.1)
Modified PLA	65.1 (+ 1.1)	2.7 (+ 0.1)	2.8 (+0.1)	109 (±0.3)	3.1 (± 0.1)	25.0 (+ 0.3)	50 (+0.1)
Unmodified PLA-wood pulp	58.7 (+ 0.5)	4.3 (+ 0.1)	2.0 (+0.1)	107 (+0.3)	5.1 (+ 0.1)	21.1 (+ 0.3)	53 (+0.1)
Modified PLA-wood pulp	61.2 (+ 0.6)	4.4 (+ 0.1)	1.8 (+0.1)	111 (+0.8)	5.2 (+ 0.2)	27.0 (+ 0.4)	53 (+0.1)
BPM PLA-wood pulp	59.8 (+0.3)	3.7 (+0.2)	2.2 (+0.1)	85.8 (+0.1)	4.0 (+0.1)	27 (+0.5)	53 (+0.1)
Silane PLA-wood pulp	71.1 (+1.0)	4.2 (+0.1)	2.7 (+0.1)	113.3 (+0.1)	4.7 (+0.1)	30.0 (+0.3)	53 (+0.1)

PLA, with the exception of the unmodified PLA-wood pulp composite.

The improvement in the impact resistance of short fiber-reinforced polymer composites can be explained in terms of an increase in the total work of fracture. This is usually due to improvements in the individual contribution of: the matrix; the fiber-matrix interface; the reinforcing fiber; and the work of friction between the fiber and the matrix.

The modification with 3-glycidoxy-propyl-trimethoxy-silane produced an increase in the impact energy to 30 J/m, whereas the impact energy of the composite modified with Paraloid® BPM-515 is similar to that of the modified PLA-wood pulp composite, i.e.: 27 J/m.

HDT

In practical terms, the Heat Deflection Temperature (HDT) of a polymer composite indicates the highest service temperature in which the stiffness of the material will not be affected by thermal energy exposure. Low HDT values are characteristic of amorphous polymers, which show low modulus at high temperature, such as PDLA. In comparison, poly(L-lactic acid) (PLLA), which has higher crystallization kinetics than PDLA, has usually a higher HDT of $\sim 64°C$.[30]

The increase in the HDT of the modified PLA blend (HDT = 50°C) can be explained in terms of its higher crystallinity (Melting behavior, crystallinity and thermal degradation temperature and XRD spectra section), if compared with neat PLA (HDT = 39°C). Harris and Lee[1] also reported enhanced HDT performance, flexural strength and modulus in injection molded PLA samples after increasing the crystallinity by nucleating agents or annealing.

The addition of wood pulp fiber increases further the HDT to 53°C. The increase corresponds to the higher modulus of the reinforcing material, which prevents the deformation of the matrix.

Morphology

Figure 12 shows the Scanning electron microscopy (SEM) micrography of wood pulp fibers with

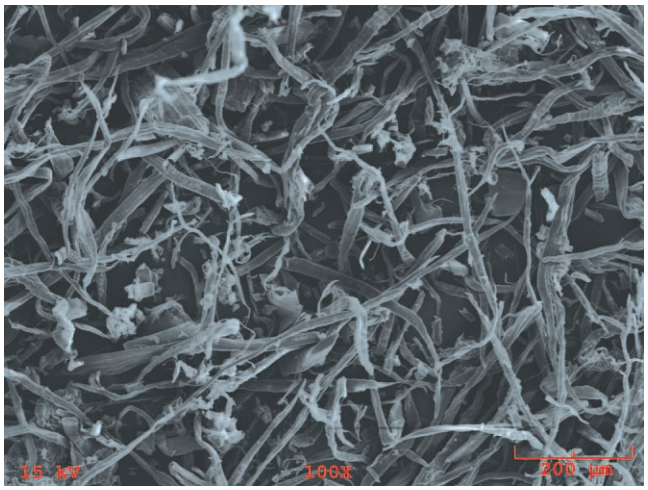

Figure 12 Scanning Electron Microscopy (SEM) micrography of wood pulp fibers (Mag. 100x). [Color figure can be viewed in the online issue, which is available at wileyonlinelibrary.com.]

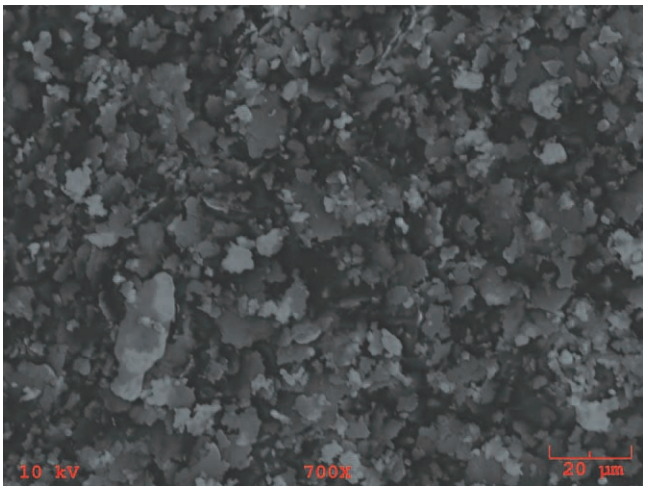

Figure 13 Scanning Electron Microscopy (SEM) micrography of wood pulp particles (Mag. 700x). [Color figure can be viewed in the online issue, which is available at wileyonlinelibrary.com.]

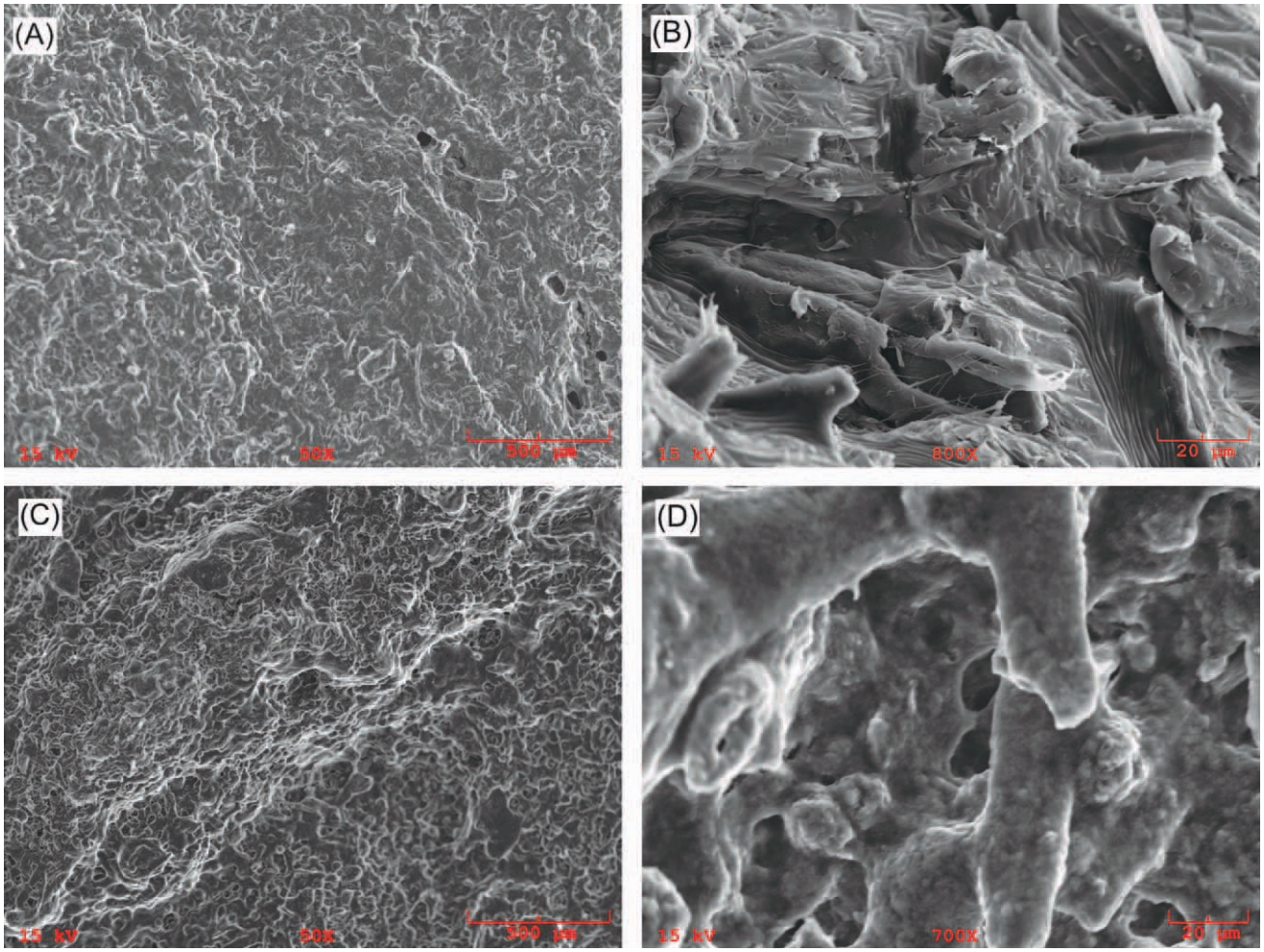

Figure 14 (A-D) Scanning Electron Microscopy (SEM) micrographies of the unmodified wood pulp-PLA composite (A) (mag. 50x) and (B) (mag. 800x), and modified wood pulp-PLA composites (C) (mag. 50 x) and (D) (mag. 700x), respectively. [Color figure can be viewed in the online issue, which is available at wileyonlinelibrary.com.]

relatively high aspect ratio (Mag. 100x). However, the Fiber Quality Analysis described in sections Fiber length determination and Fiber length analysis suggests that nearly 2.5% of the reinforcing material analyzed has a length of 50 μm or less. This small fraction of reinforcing material has a lower aspect ratio, which resembles round wood pulp particles, rather than fiber rods, as shown in Figure 13 (Mag. 700x).

Figure 14 (A–D) show the fracture surface of the unmodified wood pulp-PLA composite (A, B) and modified wood pulp-PLA composites (C, D), respectively.

The occurrence of fiber pull-outs in the fractured surface of the unmodified wood pulp-PLA composite (Fig. 14 A,B) confirm the lack of fiber-matrix interfacial adhesion, possibly because of the high content of hemicelluloses and lignin in the wood pulp fibers (Chemical composition of the fiber section), which restricts interfacial interactions, as well as the wetting of the fibers by the liquid matrix.[31]

Figure 14 C,D suggest that the modification promotes enhanced fiber-matrix adhesion since there are not so many fiber pull-outs in the fractured surface of the modified PLA-wood pulp composite. In addition, the fibers appear to be completely wetted by the matrix. The matrix shows a single and continuous phase, meaning that N,N′-(*o*-phenylene)dimalemide and 2,2′dithiobis(benzothiazole) are compatible with PLA.

CONCLUSIONS

The effect of very small amounts of N′-(*o*-phenylene) dimalemide (0.75 wt %) and 2,2′-dithiobis(benzothiazole) (0.1 wt %), on the mechanical and thermal properties of poly(D-,L-lactic acid) (PDLA) and PDLA-wood pulp fiber-reinforced composites (20 vol %) produced by injection molding was investigated.

Preliminary characterization of the wood pulp showed a mixture of wood fibers and wood particles

with different aspect ratios and fiber length, this latter between 50 and 549 μm. The amount of α-cellulose in the wood pulp fibers is near to that of the hemicelluloses (41 wt %), possibly due to the use of mixed sources to produce the pulp.

Reactive extrusion of PLA by N′-(*o*-phenylene)dimalemide and 2,2′-dithiobis(benzothiazole) produced a depression in the melting temperature (T_m) and an increase in the thermal resistance.

In addition, the modification produced an increase in the tensile strength and modulus, and an improvement in the percent crystallinity (X_c) measured by means of Differential Scanning Calorimetry (DSC). The increase in the crystallinity was confirmed by X-ray Diffraction (XRD) analysis and it explains the increase in the Heat Deflection Temperature (HDT), impact resistance, flexural strength and modulus of the modified PLA blend. The addition of wood pulp fibers to the modified PLA blend increased the HDT from 39 to 53°C.

Improved tensile strength values may be expected for the modified PLA-wood pulp composite if higher amounts of N′-(*o*-phenylene)dimalemide and 2,2′ dithiobis(benzothiazole) are used.

Fourier-Transform infrared spectroscopy (FTIR) analysis suggests that the probable mechanism of adhesion during the modification involves the creation of hydrogen bonds, and a new thiol ester and/or ester bond.

Finally, reactive extrusion of commercially available poly(lactic acid) (PLA) by means of N′-(*o*-phenylene)dimalemide and 2,2′-dithiobis(benzothiazole) is a simple, low cost and alternative method to the use of physical nucleating agents or annealing for the enhancement of the crystallinity, Heat Deflection Temperature (HDT), impact energy, tensile strength and modulus of PLA.

The authors thank the Dow Chemical Company (PA) for providing the samples, George Kretschmann (Department of Geology, University of Toronto), and Matthew Nejati (Faculty of Applied Science and Engineering, University of Toronto) for their assistance in the characterization of the samples.

References

1. Harris, A. M.; Lee, E. C. J Appl Polym Sci 2008, 107, 2246.
2. Miyata, T.; Masuko, T. Polymer 1998, 39, 5515.
3. Sain, M.; Lacok, J.; Beniska, J.; Khunova, V. Kaut Gummi Kunstst 1988, 41, 895.
4. Sain, M.; Kokta, B. V. J Adhes Sci Technol 1993, 7, 743.
5. Khunova, V.; Sain, M. Angew Makromol Chem 1995, 225, 11.
6. Sain, M.; Kokta, B. V. J Appl Polym Sci 1994, 54, 1545.
7. Xanthos, M. Polym Eng Sci 1988, 28, 1392.
8. Xian, X. J.; Choy, C. L. J Reinf Plast Compos 1994, 13, 1135.
9. Dinakaran, K.; Kumar, R. S.; Alagar, M. Mater Manuf Process 2005, 20, 299.
10. Sain, M. M.; Hudec, I.; Beniska, J.; Rosner, P. Mater Sci Eng A 1989, 108, 63.
11. Sain, M. Canada Patent 2350112, 2004.
12. Byrne, F.; Ward, P.; Kennedy, J.; Imaz, N.; Hughes, D.; Dowling, D. J Polym Environ 2009, 17, 28.
13. Swan, B. Svensk Papperstidn 1965, 68, 791.
14. Valadez-Gonzalez, A.; Cervantes-Uc, J. M.; Olayo, R.; Herrera-Franco, P. J Compos Part B 1999, 30, 309.
15. Garlotta, D. J Polym Environ 2001, 9, 63.
16. Bos, H.; Van Den Oever, M.; Peters, O. J Mater Sci 2002, 37, 1683.
17. Matthews, F. L.; Rawlings, R. D. In Composite Materials: Engineering and Science; Matthews, F. L., Rawlings, R. D., Ed.; CRC Press: Boca Raton, 2000; Chapter 10.
18. Liu, B.; Jiang, L.; Zhang, J. J Polym Environ 2011, 19, 239.
19. Yi-Zhuang, X.; Wen-Xiu, S.; Wei-Hong, L.; Xian-Bo, H.; Hai-Bo, Z.; Shi-Fu, W.; Fei, Z.; Xin-Xiang, Z.; Jin-Guang, W.; Duan-Fu, X.; Guang-Xian, X. J Appl Polym Sci 2000, 77, 2685.
20. Kholodovych, V.; Welsh, W. In Physical Properties of Polymers Handbook; Mark, J. E., Ed.; Springer: Cincinnati 2007, Chapter 54.
21. Park, J.; Lee, D.; Yoo, E.; Im, S.; Kim, S.; Kim, Y. Korea Polym J 1999, 7, 93.
22. Richardson, A.; Ward, I. M. J Polym Sci 1981, 19, 1549.
23. Henton, D. E.; Gruber, P.; Lunt, J.; Randall, J. In Natural Fibres, Biopolymers and Their Composites; Mohanty, A. K.; Mirsa, M.; Drzal, L. T., Ed.; CRC Press: Boca Raton, 2005; Chapter 16.
24. Braun, B.; Dorgan, J.; Knauss, D. J Polym Environ 2006, 14, 49.
25. El-Hosseiny, F.; Page, D. H. Fibre Sci Technol 1975, 8, 21.
26. Baltazar-Y-Jimenez, A.; Juntaro, J.; Bismarck, A. J. Biobased Mater Bioenergy 2008, 2, 264.
27. Tsuchiya, Y.; Sumi, K. J Appl Polym Sci 2003 1970, 14.
28. Nyquist, R. A.; Potts, W. J Spectrochim Acta 1959, 15, 514.
29. Trindade, W. G.; Hoareau, W.; Megiatto, J. D.; Razera, I. A. T.; Castellan, A.; Frollini, E. Biomacromolecules 2005, 6, 2485.
30. Huda, M. S.; Drzal, L. T.; Mohanty, A. K.; Misra, M. Compos Sci Tech 2008, 68, 424.
31. Bledzki, A. K.; Gassan, J. Prog Polym Sci 1999, 24, 221.